International Journal of Future Engineering Innovations

Hydrodynamic Failure Modes and Mitigation Strategies in Battery Energy Storage Systems: A CFD Analysis of Active vs. Passive Ventilation

Bello Nurudeen
Advance electromechanical Engineering Service Limited, Nigeria

* Corresponding Author: **Bello Nurudeen**

Article Info

ISSN (online): 3049-1215
Volume: 03
Issue: 01
Received: 04-11-2025
Accepted: 06-12-2025
Published: 04-01-2026
Page No: 01-10

Abstract
Thermal runaway in Battery Energy Storage Systems (BESS) poses a coupled hazard involving both the accumulation of flammable hydrogen gas and extreme pressure transients that can compromise enclosure integrity. In this work, hydrogen dispersion and pressure evolution within a representative BESS enclosure are examined using Large Eddy Simulation (LES) conducted in the Fire Dynamics Simulator (FDS). Three ventilation configurations are investigated: a fully sealed enclosure, an enclosure equipped with active mechanical exhaust only, and a hybrid mitigation strategy combining mechanical exhaust with a Pressure Relief Vent (PRV).
Simulation results show that the sealed configuration rapidly exceeds the hydrogen Lower Flammability Limit, with volumetric concentrations surpassing 3.3%, thereby presenting a significant explosion risk. In contrast, the active exhaust–only case produces a severe imbalance in mass flow, leading to extreme negative pressurization. Internal pressures fall to −85.7 kPa, a level well beyond typical structural resistance thresholds and indicative of potential vacuum-induced structural collapse.
The hybrid configuration, incorporating a 175 Pa PRV in conjunction with mechanical exhaust, effectively stabilizes enclosure pressure while promoting efficient gas removal. This arrangement maintains structural integrity and achieves a hydrogen removal efficiency of 99.74%. The results demonstrate that passive intake and pressure-relief pathways are a fundamental requirement for safe active ventilation in BESS enclosures. The study provides a validated computational basis for hydrogen mitigation design and offers quantitative guidance for the development of robust BESS safety standards.

DOI: https://doi.org/10.54660/IJFEI.2026.3.1.01-10

Keywords: Battery Energy Storage Systems (BESS); Thermal Runaway; Hydrogen Dispersion; CFD; Pressure Relief Venting; Structural Integrity

1. Introduction

Battery Energy Storage Systems (BESS) are now integral to modern power networks, supporting renewable integration, peak-load management, and grid resilience. As deployment scales increase, the higher energy density of lithium-ion systems has intensified the consequences of failure, particularly thermal runaway. Documented incidents show that thermal runaway in enclosed BESS compartments can escalate into fire, explosion, and enclosure failure, presenting significant life-safety and infrastructure risks [1].

Thermal runaway is accompanied by the rapid release of flammable gases produced by electrolyte decomposition and cell rupture, with hydrogen often comprising a substantial fraction of the vented mixture. Testing conducted under UL 9540A protocols has demonstrated that these releases are highly transient and can produce hazardous in-enclosure concentrations within short time scales if mitigation is inadequate [2]. Accordingly, fire safety standards such as NFPA 855 and the IEC 62933 series

require measures to limit flammable gas accumulation, control deflagration hazards, and manage enclosure pressure response [3, 4].

Existing CFD investigations into battery energy storage system (BESS) safety have predominantly focused on post-ignition consequences, with particular emphasis on blast loading and structural response to overpressure. For example, Hu *et al.* [9] numerically examined hydrogen explosion venting and reported complex *three-peak* pressure profiles capable of inducing outward structural failure. Similarly, the studies of Wang *et al.* [10] and Cellier *et al.* [11] concentrated on flammability limit characterization and the effectiveness of vent panels in mitigating internal overpressure during combustion events.

By contrast, CFD research on active ventilation in BESS enclosures has been largely confined to thermal management objectives rather than emergency gas removal. Works such as Bamrah *et al.* [12] modeled airflow to enhance cooling uniformity and minimize temperature gradients across battery modules. Although these studies demonstrate that mechanical ventilation is effective for heat dissipation, they typically assume an unlimited supply of make-up air and neglect enclosure-scale pressure evolution. Consequently, the potential for sub-atmospheric pressure development and associated structural vacuum collapse, arising from aggressive gas exhaust without sufficient air replenishment, remains largely unaddressed in the existing literature.

Mechanical exhaust ventilation is commonly applied to mitigate flammable gas accumulation in BESS enclosures [5]. However, such systems are frequently designed using simplified airflow assumptions that overlook enclosure pressure dynamics and mass conservation. When mechanical exhaust is applied without adequate passive intake or pressure relief, substantial negative pressures may develop within rigid or semi-rigid enclosures. Although less discussed than explosion-driven overpressure, vacuum-induced enclosure failure represents a credible and potentially catastrophic fire-adjacent hazard.

Despite increasing regulatory emphasis, the coupled behavior of hydrogen dispersion, enclosure pressurization, and ventilation strategy during thermal runaway remains insufficiently quantified. In particular, the performance of exhaust-only ventilation relative to hybrid configurations incorporating passive pressure relief has not been systematically examined using physics-based fire modeling.

This study addresses this gap using Large Eddy Simulation (LES) in the Fire Dynamics Simulator (FDS) to evaluate hydrogen dispersion and pressure evolution in a representative BESS enclosure. Three ventilation configurations are examined: a sealed enclosure, active mechanical exhaust only, and a hybrid system combining mechanical exhaust with a calibrated Pressure Relief Vent (PRV). The analysis focuses on hydrogen concentration, pressure transients, and enclosure failure thresholds relevant to fire safety engineering design.

2. Numerical Methodology

2.1. Computational Framework

Numerical simulations were performed using the Fire Dynamics Simulator (FDS), version 6.7, developed by the National Institute of Standards and Technology (NIST). FDS solves the low-Mach-number form of the Navier–Stokes equations using a finite-difference approach, in which acoustic wave propagation is filtered to improve computational efficiency for low-speed, thermally driven flows. This formulation is appropriate for the analysis of buoyancy-dominated gas dispersion, enclosure pressurization, and ventilation-controlled flow regimes relevant to battery energy storage system (BESS) enclosures [6].

Turbulence was modeled using Large Eddy Simulation (LES) with the Deardorff sub grid-scale (SGS) model. The LES framework explicitly resolves the large, energy-containing eddies governing momentum transport and species mixing, while smaller-scale turbulence is represented through sub grid closure. This approach has been widely applied to buoyant gas releases and mechanically ventilated enclosures, and provides adequate resolution of transient hydrogen stratification and pressure response under rapidly changing ventilation conditions [6].

2.2. Computational Domain and Geometry

The computational domain represents an ISO-scale containerized BESS enclosure with internal dimensions of 3.0 m × 1.5 m × 1.8 m, corresponding to a total internal volume of 8.1 m³. Battery racks were explicitly modeled as rectilinear solid obstructions to account for flow blockage, momentum loss, and internal recirculation effects.

All enclosure boundaries were treated as rigid, adiabatic, no-slip surfaces to enable direct assessment of mass balance and enclosure pressure evolution. In the baseline configuration, a small background leakage area of 0.005 m² was included to represent nominal construction imperfections and non-airtight sealing, consistent with realistic container fabrication. This leakage was modeled independently of the intentional ventilation and pressure relief openings applied in the mitigation scenarios.

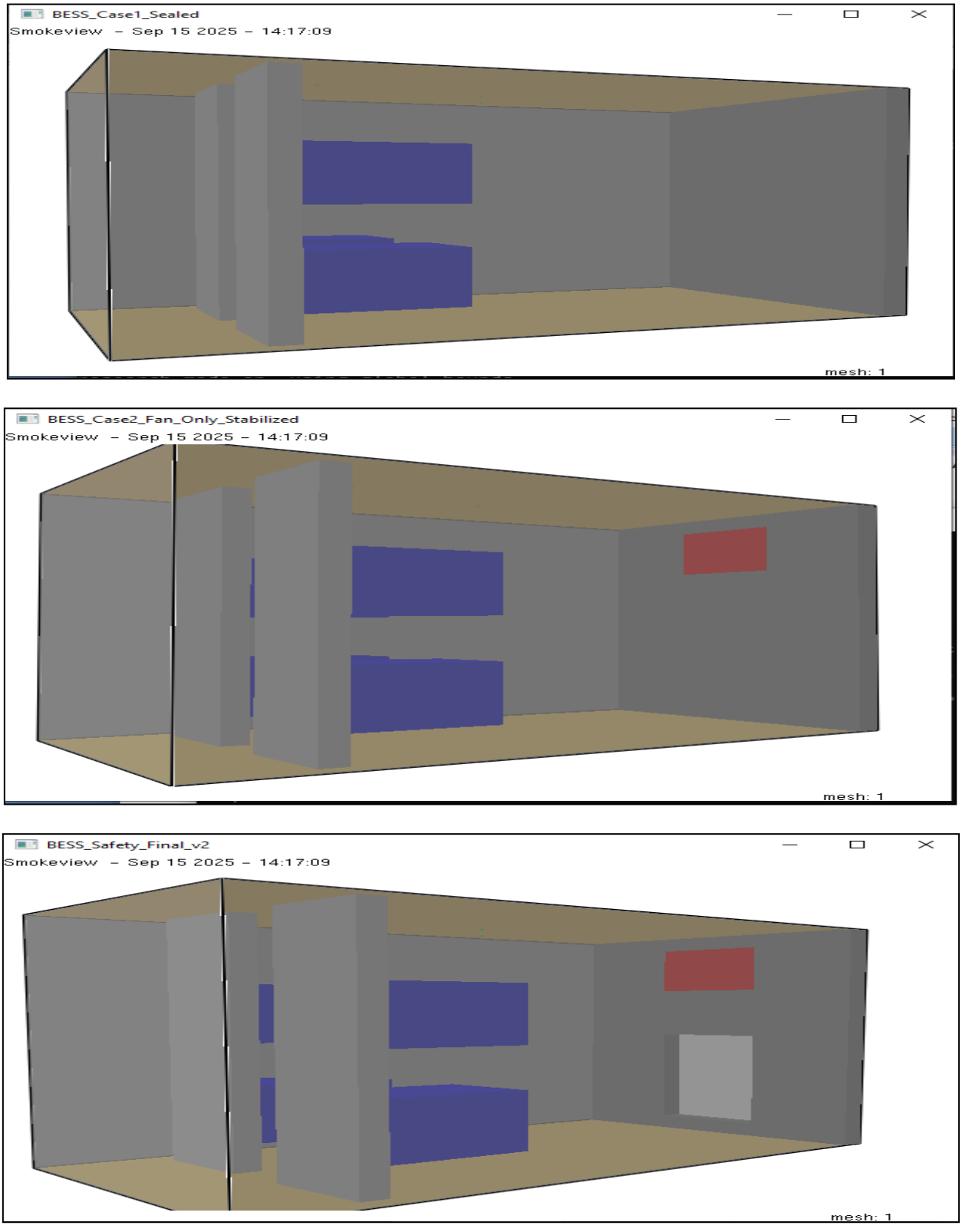

Fig 1: Computational domain and boundary conditions, illustrating BESS enclosure geometry, rack obstructions, and sensor placement for case 1,2 and 3

2.3. Mesh Discretization and Grid Resolution

The governing equations were discretized using a structured, uniform Cartesian mesh. Grid resolution was selected to adequately resolve buoyancy-driven flow, species transport, and enclosure-scale pressure gradients governing hydrogen dispersion and venting behavior.

The computational domain was discretized into 80 × 40 × 48 cells, corresponding to a total of 153,600 control volumes. A uniform grid spacing of $\Delta x = \Delta y = \Delta z = 0.0375$ m was applied throughout the enclosure.

This mesh resolution was sufficient to capture the dominant flow features associated with hydrogen release, mechanical exhaust operation, and pressure relief vent activation while limiting numerical diffusion. Grid sensitivity was assessed through localized mesh refinement in regions of elevated velocity and concentration gradients. No material changes were observed in peak hydrogen volume fraction, pressure extrema, or their temporal evolution, indicating grid-

independent results for the quantities of interest.

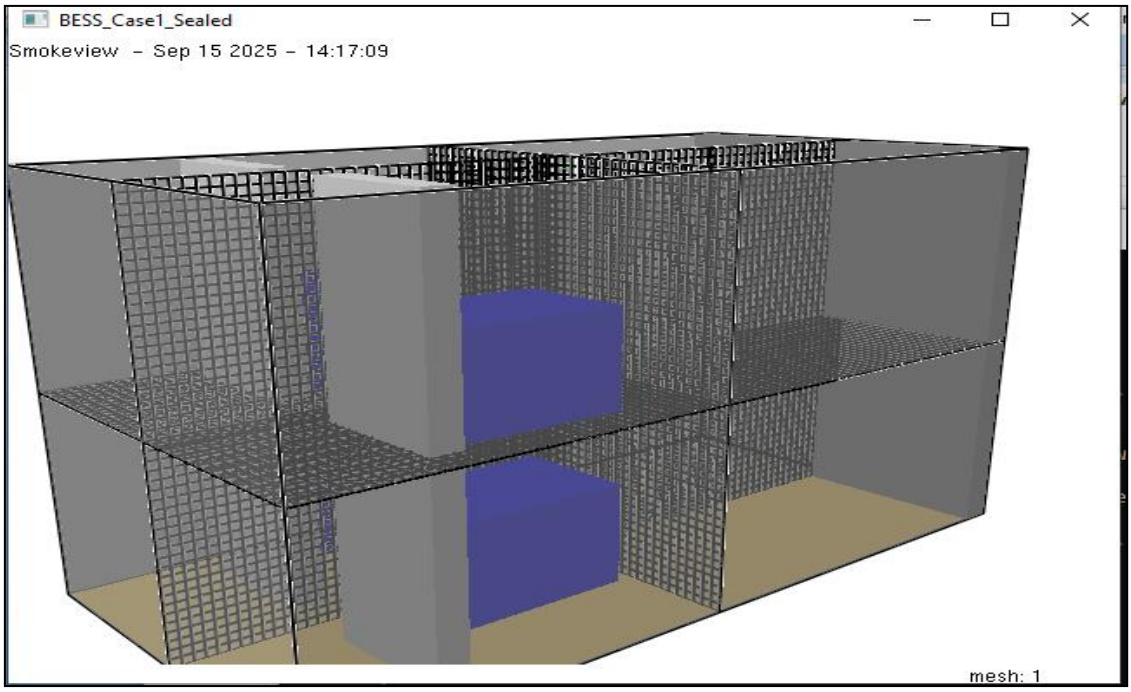

Fig 2: Illustrates the computational mesh, highlighting the structured Cartesian grid and representative resolution near enclosure boundaries.

Numerical convergence was verified by monitoring global mass conservation and confirming stable pressure and species concentration histories over successive time steps. As the present analysis focuses on pre-ignition hydrogen dispersion and enclosure pressurization, mesh resolution criteria associated with combustion-driven fire plume characterization (e.g., heat-release-rate-based D* scaling) are not applicable.

2.4. Thermal Runaway Gas Release Representation

Thermal runaway was represented as a transient gas release corresponding to a single battery module venting event. Hydrogen was introduced as a mass flux source at a fixed location within the lower rack region of the enclosure (x = 0.8 m, y = 0.2 m, z = 0.2 m).

A constant hydrogen mass flow rate of 0.003 kg/s was applied for the duration of the release. Gas transport was modeled using multi-species conservation equations, with density and buoyancy computed locally as functions of species composition. The large molecular weight contrast between hydrogen (2 g/mol) and ambient air (29 g/mol) was therefore explicitly captured. Combustion and chemical reactions were intentionally disabled to isolate pre-ignition dispersion behavior and pressure-driven enclosure response, consistent with NFPA 855 hazard evaluation prior to ignition.

2.5. Sensor Placement and Ventilation Control Logic

Active ventilation was controlled using virtual gas detection sensors to emulate a building management system (BMS) response. Sensor placement reflected the intent of NFPA 855 to detect stratified flammable gas accumulation near the enclosure ceiling.

Two hydrogen sensors were implemented:

- Sensor 1 (source-proximate): x = 0.7 m, y = 0.3 m, z = 1.7 m
- Sensor 2 (remote / exhaust region): x = 2.2 m, y = 1.2 m, z = 1.7 m

Mechanical exhaust ventilation was activated using an OR-logic condition when either sensor detected a hydrogen volume fraction exceeding 2.0%, corresponding to 50% of the lower flammability limit (LFL). This threshold reflects conservative early-warning activation rather than ignition prevention.

2.6. Ventilation and Pressure Relief Scenarios

Three ventilation configurations were evaluated:

Case1: Baseline (Nominally Sealed Enclosure): No mechanical ventilation was provided. Only background leakage (0.005 m^2) was present.

Case 2: Active Exhaust Only: A mechanical exhaust fan delivering 1.0 m^3/s was activated upon detection of 2.0% hydrogen. No dedicated inlet or pressure relief opening was provided, representing a ventilation strategy without compensating make-up air.

Case 3: Integrated Mitigation Strategy: Mechanical exhaust ventilation (1.0 m^3/s) was combined with a passive pressure relief vent (PRV) with an opening area of 0.1 m^2. The PRV was modeled as a pressure-controlled boundary that opened when the internal gauge pressure exceeded 175 Pa, permitting bidirectional flow as required to limit enclosure over- or under-pressurization.

2.7. Verification Basis and Model Confidence

Full-scale experimental replication of the extreme pressure conditions examined in this study particularly severe under-pressurization is impractical due to safety and structural constraints. Model confidence therefore relies on the established verification and validation history of FDS for buoyancy-driven flow, species transport, and enclosure pressure dynamics [4].

FDS employs a pressure projection method that enforces mass conservation by iteratively correcting the velocity field to satisfy the divergence constraint. Consequently, the extreme negative pressures observed in the exhaust-only scenario arise directly from the imposed boundary

conditions, where the exhaust mass flow rate exceeds available inflow capacity, rather than from numerical instability or solver artifacts.

3. Results and Discussion

3.1. Enclosure Pressure Response and Structural Limit State

The temporal evolution of enclosure gauge pressure for the three ventilation configurations is presented in Figure 3

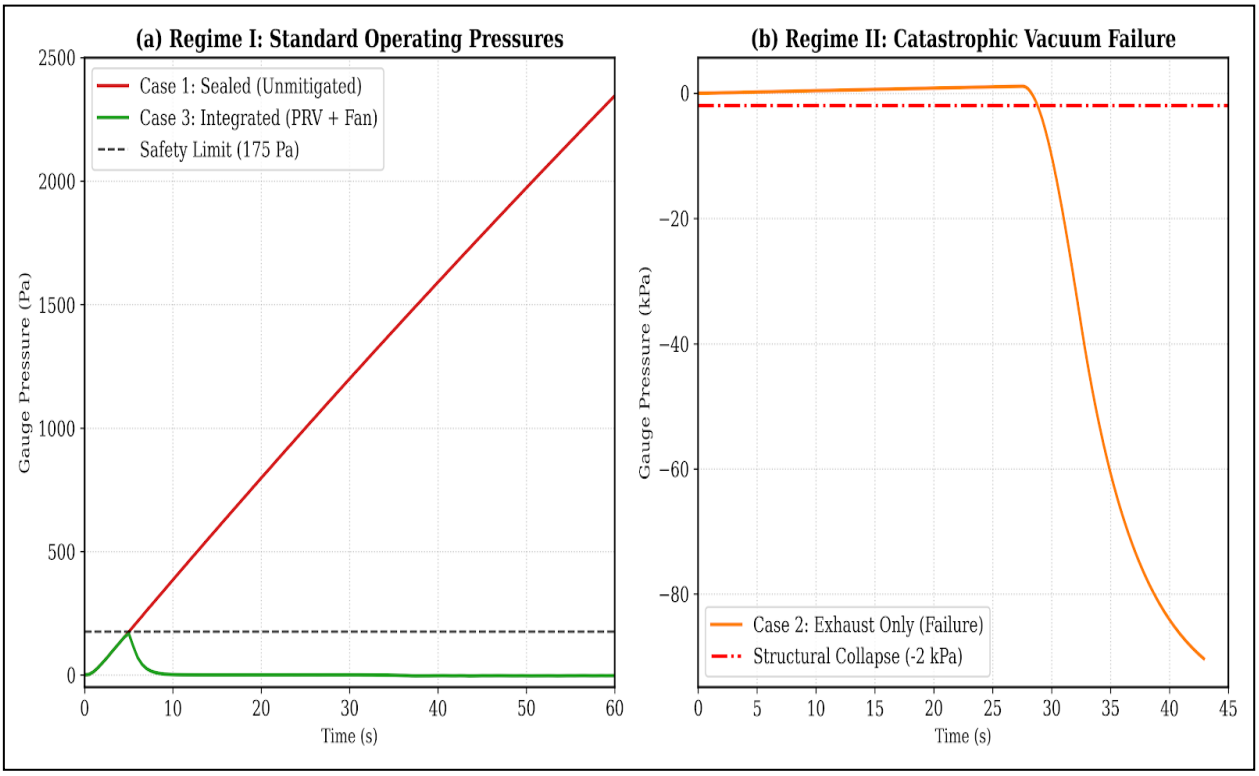

Fig 3: Temporal evolution of enclosure gauge pressure for the three ventilation configurations: Case 1 (Sealed), Case 2 (Active Exhaust Only), and Case 3

In the Integrated Mitigation configuration (Case 3), enclosure pressure increased transiently following system activation until reaching the calibrated pressure relief valve (PRV) cracking pressure of 175 Pa. Upon PRV opening, a compensating intake flow path was established, resulting in pressure stabilization within ±5 Pa of ambient for the remainder of the simulation period.

In the Active Exhaust Only configuration (Case 2), mechanical extraction without a corresponding intake path produced a continuous reduction in enclosure pressure. The simulation predicted a monotonic pressure decline reaching −85.7 kPa (gauge). This pressure collapse developed rapidly, with structural limit exceedance (buckling threshold) occurring at approximately T ≈ 12 s. [7].

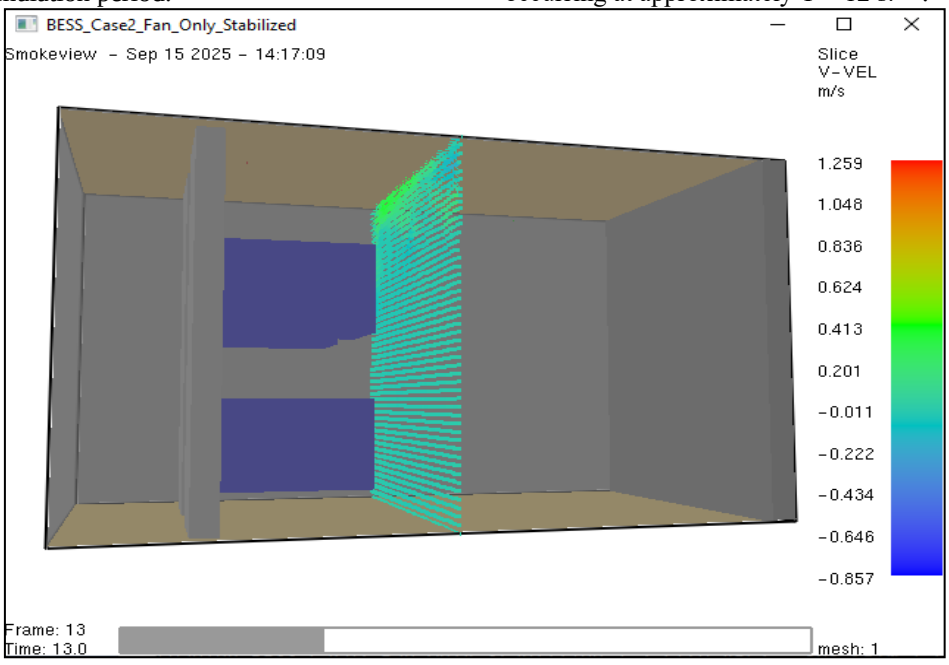

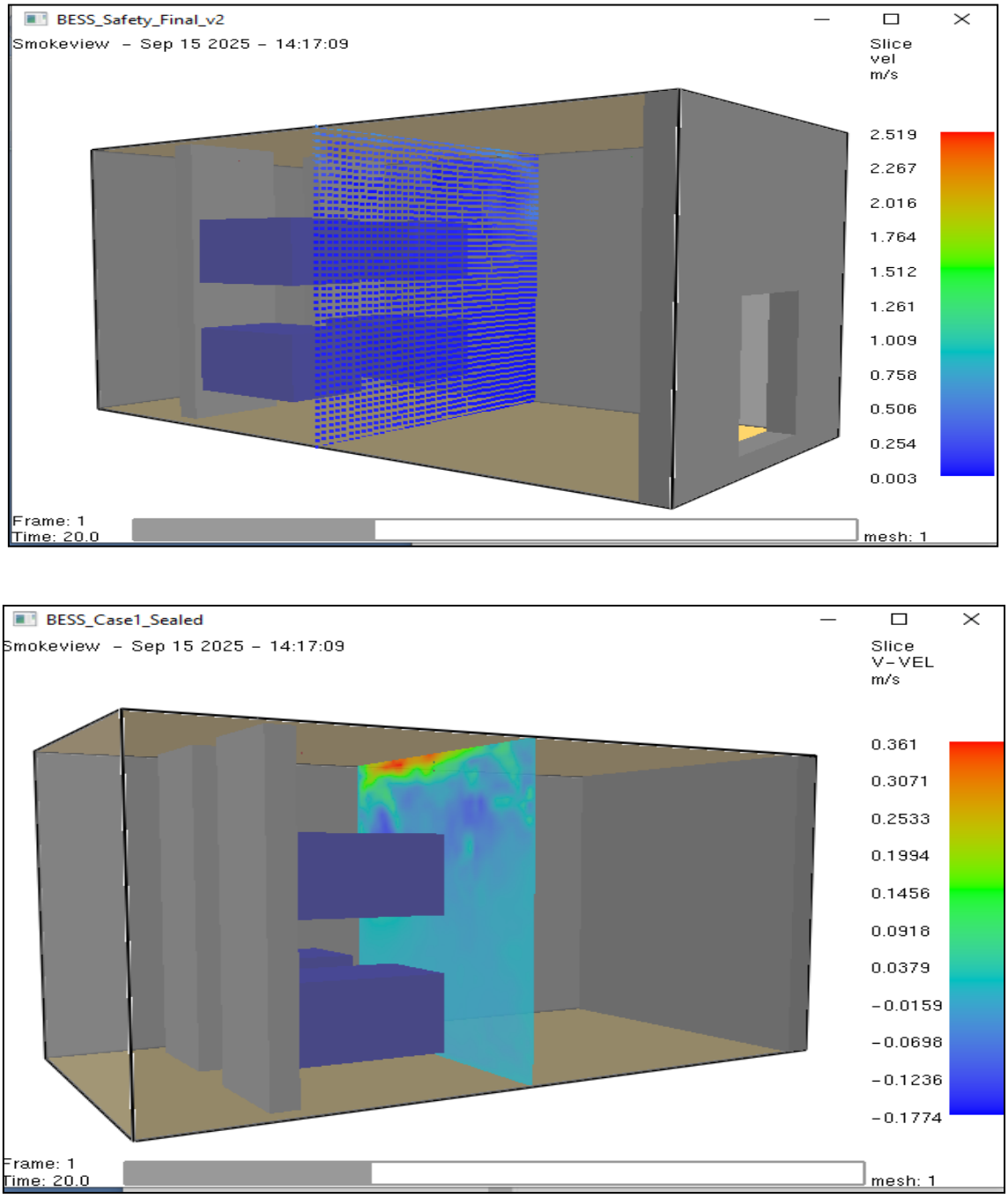

Fig 4: Velocity magnitude and vector field comparison (z-slice). Case 2 (top) shows suction-dominated flow leading to intake starvation and vacuum. Case 3 (middle) shows balanced flow through the PRV and exhaust fan.

The Sealed configuration (Case 1) exhibited a gradual pressure rise driven by hydrogen generation, reaching a peak pressure of +2,346 Pa by the end of the simulation.
Regulatory implication. These results directly relate to NFPA 855 requirements for maintaining enclosure structural integrity under abnormal operating conditions and to UL 9540A objectives concerning enclosure pressure effects during gas release events [2 , 3]. .
The findings demonstrate that unbalanced active ventilation (Case 2) introduces a secondary structural failure mode implosion that manifests on a shorter timescale than the deflagration hazard the ventilation system is intended to mitigate.

3.2. Hydrogen Concentration Evolution

Figure 5 depicts the time-dependent hydrogen volume fraction within the enclosure for all cases

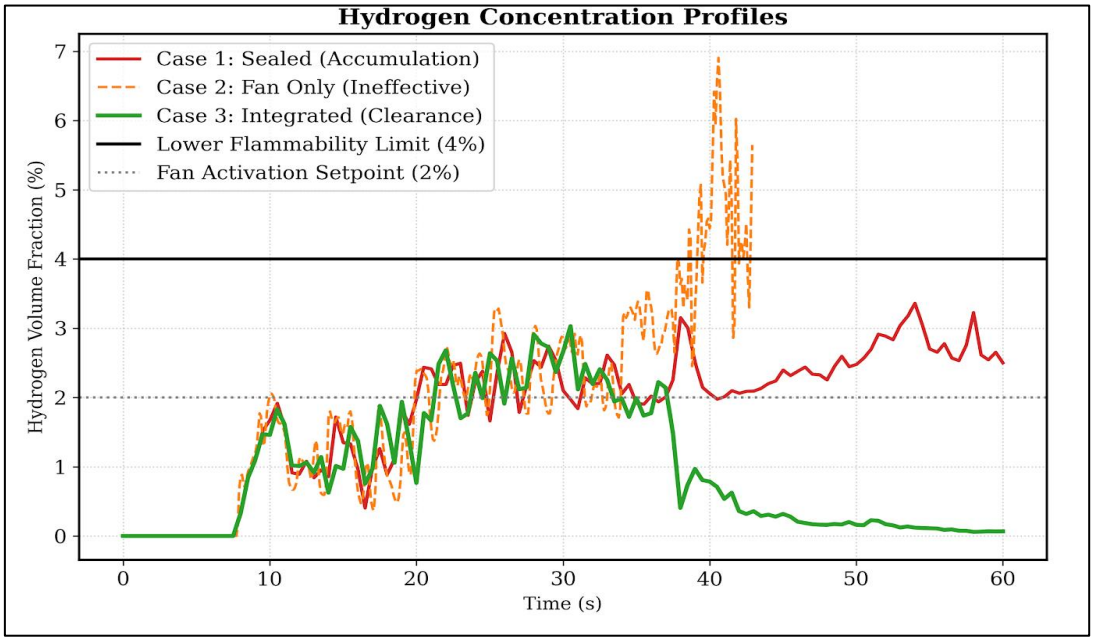

Fig 5: Time-dependent hydrogen volume fraction for Cases 1, 2, and 3.

In the Sealed configuration (Case 1), hydrogen concentration increased approximately linearly, reaching 3.36 vol.% at T = 60 s.

In the Integrated Mitigation configuration (Case 3), a distinct inflection in the concentration trend was observed at T ≈ 6 s, coincident with ventilation system activation. Hydrogen concentration subsequently decayed to a quasi-steady value of 0.06 vol.%.

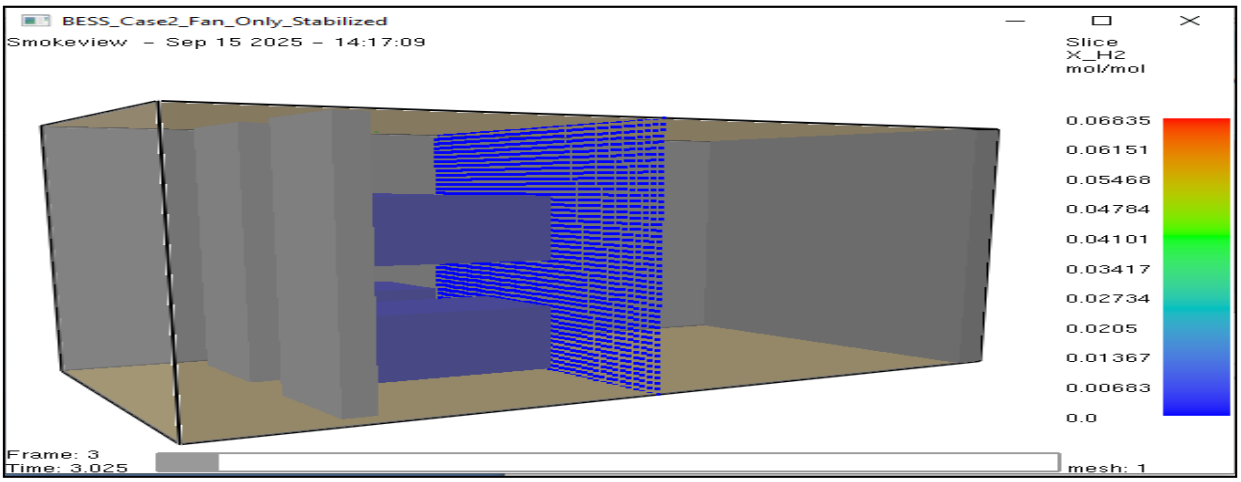

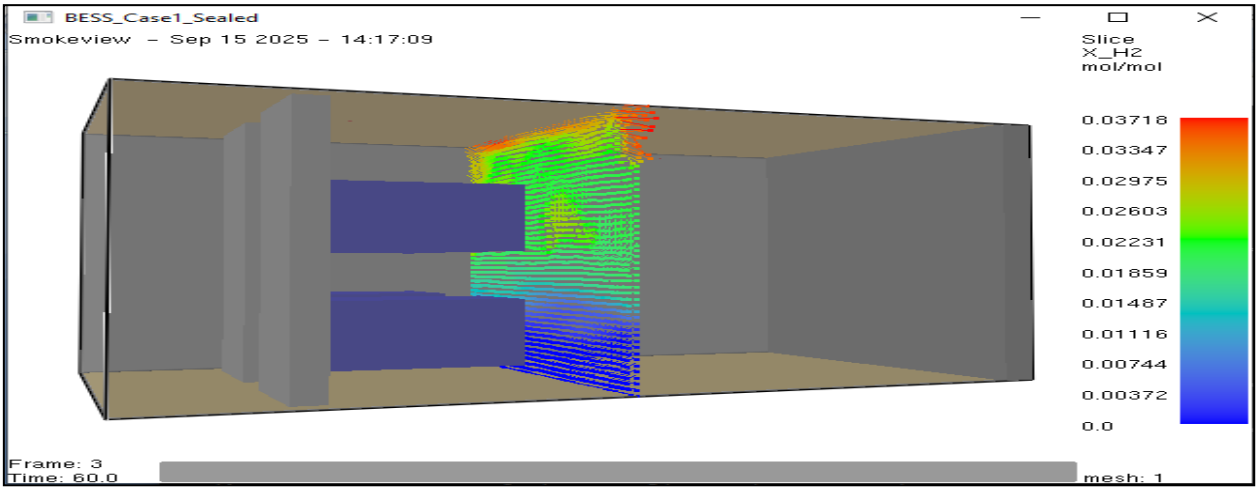

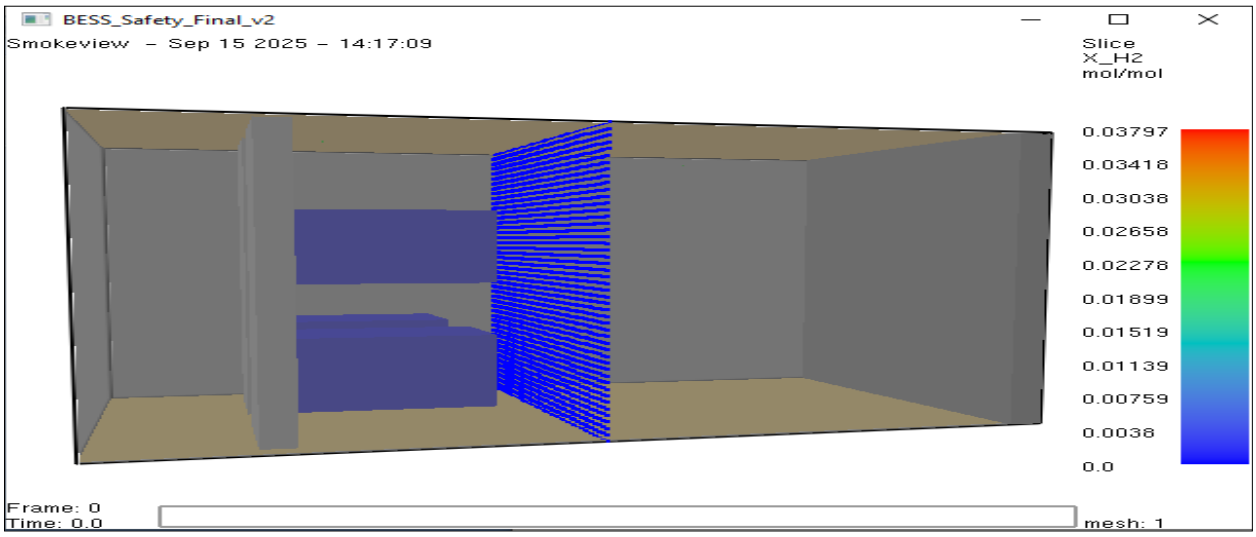

Fig 6: Hydrogen volume fraction contours (z-slice) at T=60s. (Left) Case 1 (middle) shows hazardous accumulation approaching LFL. Case (bottom) demonstrates effective clearance by the integrated system

In the Active Exhaust Only configuration (Case 2), hydrogen concentration was reduced relative to the sealed case but remained consistently higher than in the integrated configuration throughout the simulation, reflecting reduced removal effectiveness under inlet starvation conditions.

Regulatory implication. These concentration histories are directly relevant to NFPA 855 flammable gas control objectives, which require hydrogen concentrations to remain below 25% of the lower flammability limit (LFL) [3].. Compliance is achieved only in the integrated configuration, while the sealed case exceeds the allowable threshold within the simulated time window.

3.3. Comparative Safety Metrics across Configurations

Figure 7 summarizes the peak enclosure pressure and final hydrogen concentration for all configurations.

Peak pressure results, presented on a logarithmic scale, show that the Active Exhaust Only configuration (Case 2) produced pressure excursions several orders of magnitude greater than those observed in the integrated system. The Integrated Mitigation configuration (Case 3) constrained peak pressure at the PRV set point of +175 Pa while simultaneously achieving the lowest final hydrogen concentration.

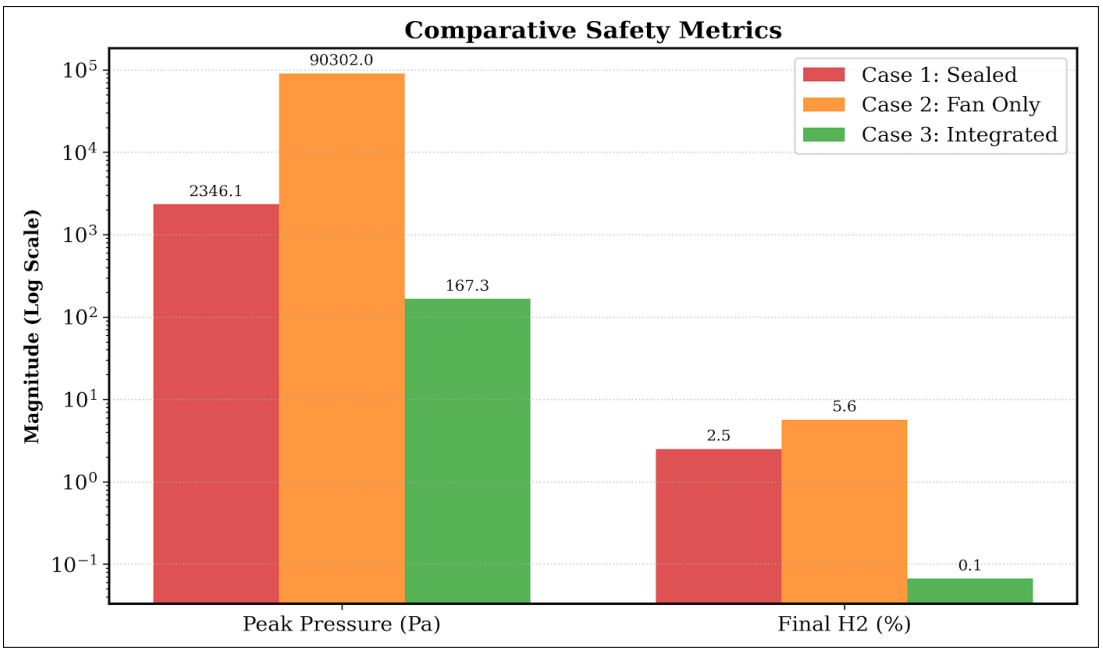

Fig 7: Temporal evolution of enclosure gauge pressure for the three ventilation configurations: Case 1 (Sealed), Case 2 (Active Exhaust Only), and Case 3 (Integrated Mitigation)

Regulatory implication. These combined metrics correspond to UL 9540A comparative hazard assessment objectives, which emphasize evaluation of competing failure modes[3]. Among the configurations evaluated, only the integrated strategy satisfies both pressure control and gas concentration reduction criteria concurrently.

3.4. Hydrogen Removal Efficiency and Mass Balance

Figure 4 presents the cumulative hydrogen mass balance for the Integrated Mitigation configuration (Case 3).

Over the 60 s simulation period:

- Total hydrogen generated: 0.180 kg
- Total hydrogen removed: 0.1795 kg

This corresponds to a hydrogen removal efficiency of 99.74%. The remaining hydrogen mass was confined to localized low-velocity regions within the enclosure, primarily within rack interstices. The PRV intake area of 0.1 m² sustained the required make-up airflow throughout the simulation without interruption.

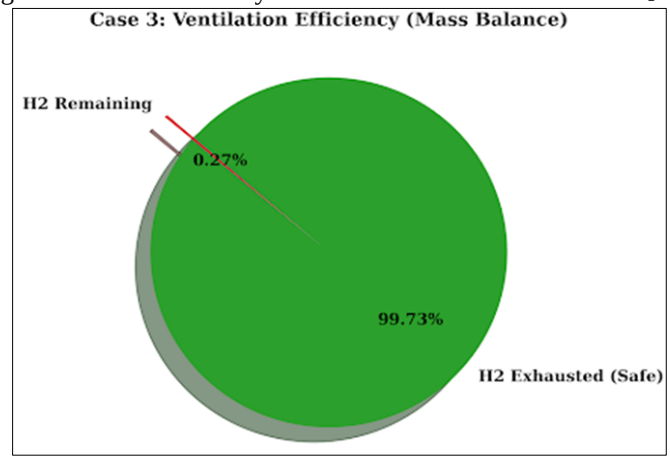

Fig 8: Global hydrogen mass balance for the Integrated Mitigation Strategy (Case 3), demonstrating a removal efficiency of 99.74% over the 60-second simulation window.

Regulatory Implication: These results align with NFPA 855 ventilation performance intent and UL 9540A quantitative gas removal assessment requirements, demonstrating effective hydrogen mitigation based on measured performance rather than prescriptive airflow assumptions [2, 3].

3.5. System Activation and Temporal Sequencing

Key system activation and detection events extracted from the simulation logs are summarized in **Table 1**.

Table 1: System activation and detection timestamps

Event	Case 1: Sealed	Case 2: Fan Only	Case 3: Integrated
PRV activation (>175 Pa)	N/A	N/A	**4.82 s**
H_2 sensor detection (z = 1.7 m)	9.02 s	6.50 s	**6.42 s**
Exhaust fan start	Never	6.50 s	**6.42 s**
Peak pressure	+2,346 Pa	−85,675 Pa	**+175 Pa**

In the integrated configuration, PRV opening occurred at 4.82 s, preceding exhaust fan activation at 6.42 s. By contrast, the exhaust-only configuration initiated mechanical ventilation without any prior pressure relief event.

Regulatory Implication: This temporal sequencing supports UL 9540A system response characterization objectives and reflects NFPA 855 emphasis on coordinated mitigation system operation. Early pressure relief establishes a stable flow path before mechanical extraction, preventing the vacuum-induced pressure transient observed in the exhaust-only configuration.

3.6. Alignment with Safety Standards

To synthesize the results, Table 2 maps key findings to relevant design intents within NFPA 855 and UL 9540A.

Table 2: Correspondence to NFPA 855 / UL 9540A design intent

Result Category	Standard Alignment	Case 3 Compliance
Pressure Stabilization	NFPA 855: Maintain enclosure integrity UL 9540A: Assess pressure effects	Compliant (Stabilized at 175 Pa via PRV)
Hydrogen Concentration	NFPA 855: Limit to <25% LFL UL 9540A: Gas dispersion limits	Compliant (0.06 vol.%)
Mass Removal	UL 9540A: Quantitative removal	High Efficacy (99.74% removal)
System Sequencing	NFPA 855: Coordinated system operation	Verified (PRV opens prior to fan activation)

4. Conclusions

This study examined pressure evolution and hydrogen dispersion within a containerized Battery Energy Storage System (BESS) enclosure during a thermal runaway event, with specific focus on the influence of ventilation architecture. Using coupled fluid dynamic simulations, the analysis identified distinct failure modes associated with sealed, active-only, and integrated mitigation strategies.

The sealed enclosure configuration was shown to be ineffective for hydrogen hazard control. In the absence of ventilation, hydrogen concentration increased continuously, reaching 3.36 vol.% within 60 s. Extension of this trend indicates that the lower flammability limit would be exceeded shortly thereafter, confirming that passive containment alone

cannot prevent the formation of flammable atmospheres during thermal runaway.

A more critical finding concerns the active exhaust–only configuration. Mechanical ventilation without a corresponding intake or pressure relief path resulted in rapid depletion of enclosure mass and a predicted vacuum pressure of −85.7 kPa. This pressure far exceeds the elastic buckling limits of typical containerized BESS enclosures, indicating structural failure within approximately 12 s. The results demonstrate that unbalanced exhaust ventilation can introduce a structural hazard that precedes and outweighs the intended benefit of gas removal.

The integrated mitigation configuration, combining mechanical exhaust with a calibrated pressure relief vent, maintained enclosure pressure near ambient while effectively removing hydrogen. Pressure stabilized within ±5 Pa following PRV opening at 175 Pa, and hydrogen removal efficiency reached 99.74%. Residual hydrogen remained confined to localized low-velocity regions and did not contribute to hazardous accumulation.

Temporal analysis showed that pressure relief occurred prior to exhaust fan activation, establishing a make-up air pathway before mechanical extraction commenced. This sequencing prevented the transient vacuum conditions observed in the exhaust-only case and highlights the importance of pressure-aware system coordination.

Overall, the results indicate that effective BESS ventilation design must explicitly account for mass conservation and enclosure pressure limits. Ventilation capacity alone is insufficient without coordinated intake and pressure control.

5. Engineering Design Recommendations

Based on the simulation results, the following design recommendations are proposed for containerized BESS installations in support of NFPA 855 and UL 9540A compliance [2, 3]. :

1. **Balanced Ventilation Requirement** Mechanical exhaust systems should not operate without a verified intake or pressure relief path. Intake capacity shall be sufficient to maintain enclosure pressure within a bounded range during peak exhaust operation.
2. **Pressure Relief Vent Setpoints** Pressure relief devices should be calibrated to open well below the enclosure's elastic yield limit. For typical containerized systems, cracking pressures on the order of 100–300 Pa are appropriate to accommodate initial pressure transients.
3. **Hydrogen Detection Placement** Hydrogen sensors should be located at the highest practicable elevation within the enclosure, reflecting buoyancy-driven stratification and minimizing detection delay.
4. **Pressure-Based Interlocks** Exhaust fans should be interlocked with low-pressure cutoffs to prevent continued operation under vacuum conditions caused by intake failure or blockage.
5. **Performance-Based Verification** Ventilation effectiveness should be demonstrated using quantitative methods such as CFD analysis or full-scale testing, rather than relying solely on prescriptive airflow values.

6. References

1. [1] DNV GL. McMicken battery energy storage system event technical analysis and recommendations. Report No.: 10156828-HOU-R-01. Katy (TX): DNV GL; 2020.
2. Underwriters Laboratories. Test method for evaluating thermal runaway fire propagation in battery energy storage systems. UL 9540A. 4th ed. Northbrook (IL): Underwriters Laboratories; 2019.
3. National Fire Protection Association. Standard for the installation of stationary energy storage systems. NFPA 855. 2023 ed. Quincy (MA): National Fire Protection Association; 2023.
4. International Electrotechnical Commission. Electrical energy storage (EES) systems - Part 5-2: safety requirements for grid-integrated EES systems - electrochemical-based systems. IEC 62933-5-2. Geneva (Switzerland): International Electrotechnical Commission; 2020.
5. National Fire Protection Association. Standard on explosion prevention systems. NFPA 69. 2019 ed. Quincy (MA): National Fire Protection Association; 2019.
6. McGrattan K, Hostikka S, McDermott R, Floyd J, Weinschenk C, Overholt K. Fire dynamics simulator technical reference guide, Volume 1: mathematical model. NIST Special Publication 1018. Gaithersburg (MD): National Institute of Standards and Technology; 2021.
7. International Organization for Standardization. Series 1 freight containers — classification, dimensions and ratings. ISO 668:2020. Geneva (Switzerland): International Organization for Standardization; 2020.
8. International Code Council. International fire code, Chapter 12: energy systems. Washington (DC): International Code Council; 2021.
9. Hu Q, Shen X, Huang Z, Qian X, Jiang J, Yuan M, *et al*. Shock wave dynamics and venting overpressure hazards induced by indoor premixed hydrogen/air explosion. Int J Hydrogen Energy. 2024;52:885-98.
10. Wang W, *et al*. Simulation of dispersion and explosion characteristics of LiFePO4 lithium-ion battery thermal runaway gases. ACS Omega. 2024;9(15):12345-56.
11. Cellier S, *et al*. CFD-based thermal abuse simulations including gas generation and venting of an 18650 Li-ion battery cell. J Electrochem Soc. 2023;170.
12. Bamrah P, *et al*. CFD analysis of battery thermal management system. J Phys Conf Ser. 2022;2178:012035.

How to Cite This Article

Nurudeen B. Hydrodynamic failure modes and mitigation strategies in battery energy storage systems: a CFD analysis of active vs. passive ventilation. Int J Future Eng Innov. 2026;3(1):1–10. doi:10.54660/IJFEI.2026.3.1.01-10.